Supplement of Atmos. Chem. Phys., 23, 12589–12607, 2023
https://doi.org/10.5194/acp-23-12589-2023-supplement

Atmospheric Chemistry and Physics
Open Access

Supplement of

Occurrence frequency of subcritical Richardson numbers assessed by global high-resolution radiosonde and ERA5 reanalysis

Jia Shao et al.

Correspondence to: Jian Zhang (zhangjian@cug.edu.cn)

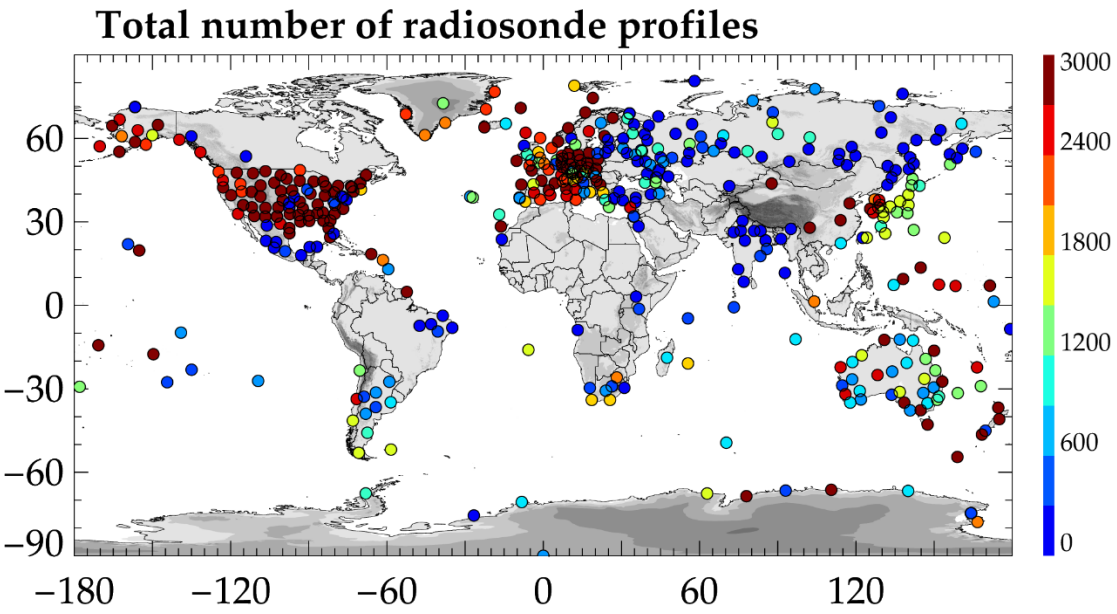

Figure S1. Total released soundings over each station.

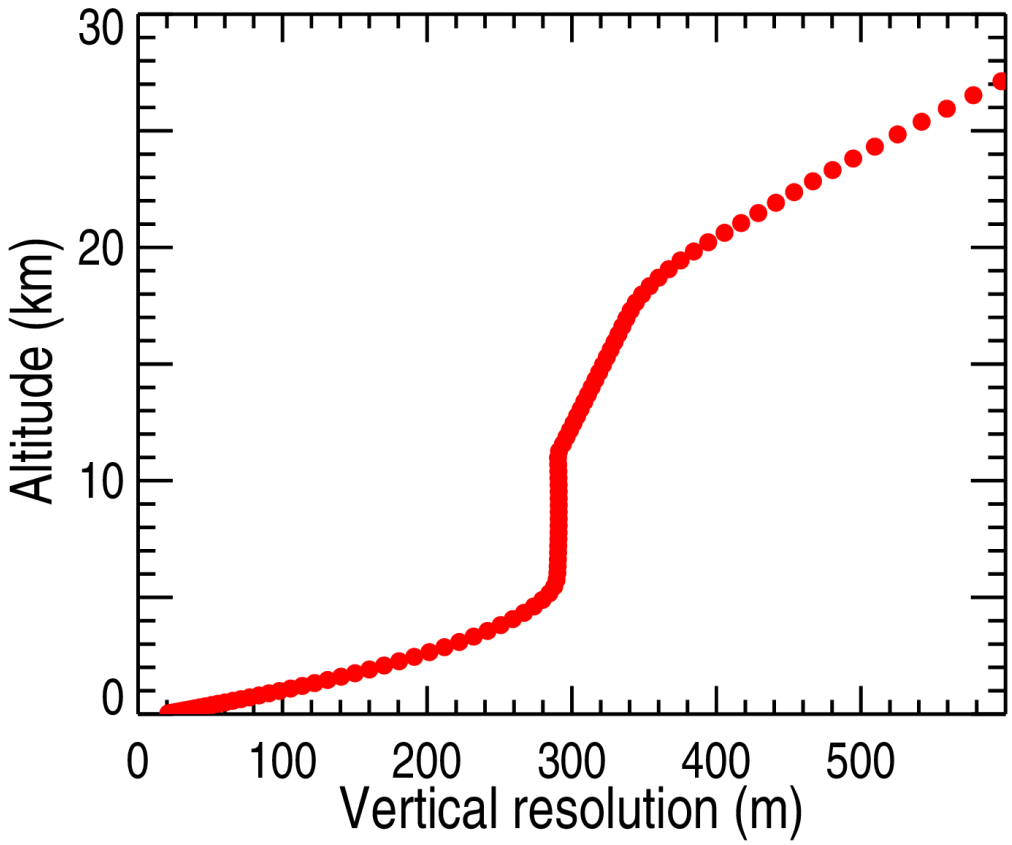

Figure S2. Vertical resolution of ERA5 at different heights.

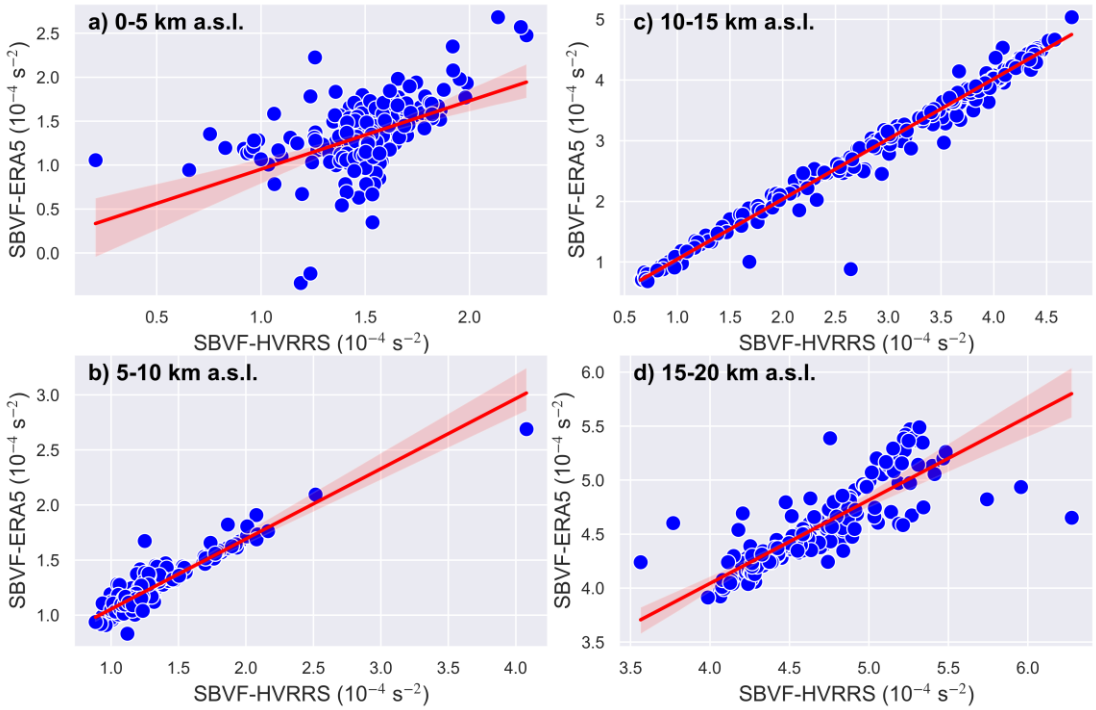

Figure S3. The joint distributions of HVRRS-retrieved and ERA5-determined squared Brunt-väisälä frequency together with the linear regression (red line) at heights of 0–5 km a.g.l. (a), 5–10 km a.g.l. (b), 10–15 km a.g.l. (c), and 15–20 km a.g.l. (d). The light red shadow denotes a significance of 95%. The Brunt-väisälä frequency is averaged during the whole study period. The ERA5 derived N^2 is spatially and temporally collocated with that of HVRRS.

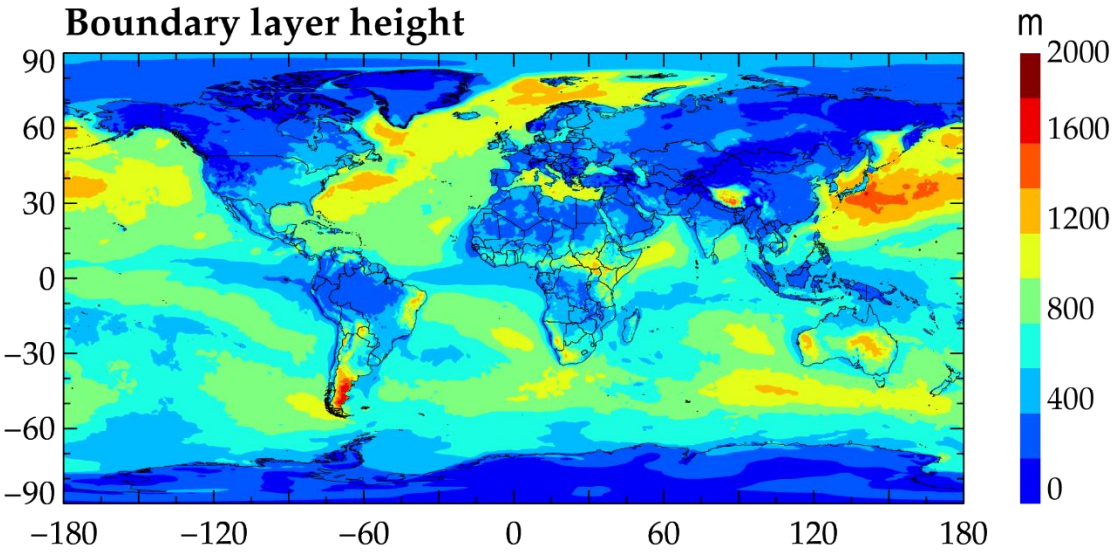

Figure S4. The averaged planetary boundary layer height during years 2017 to 2022.

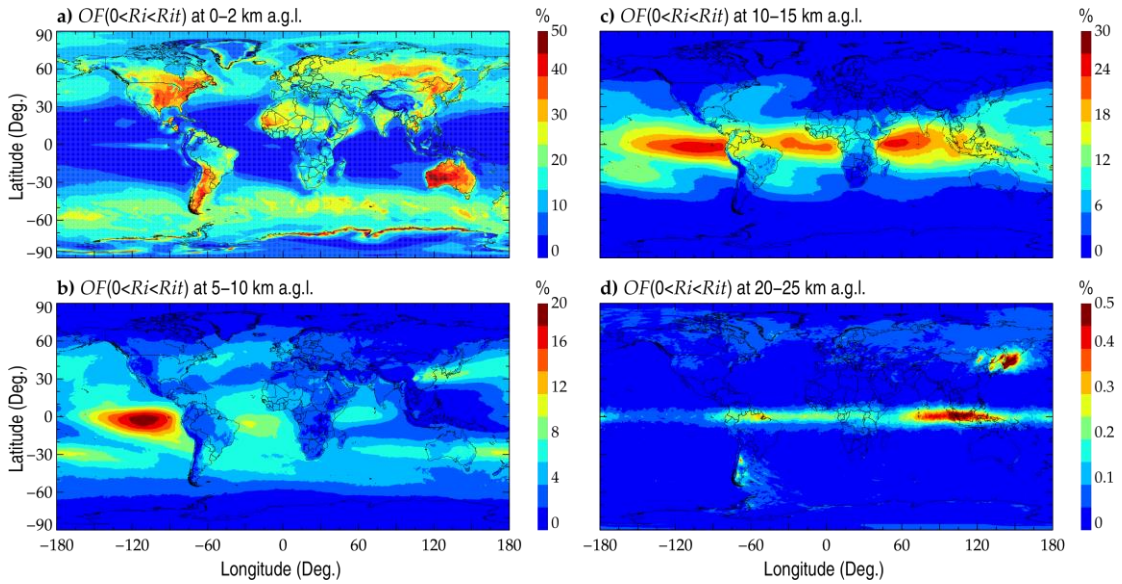

Figure S5. The spatial distribution of the mean *OF*(0<*Ri*<*Rit*) in ERA5 reanalysis at 0–2 km a.g.l. (a), 5–10 km a.g.l. (b), 10–15 km a.g.l. (c), and 20–25 km a.g.l. (d). Note that *Rit* is set to 1.

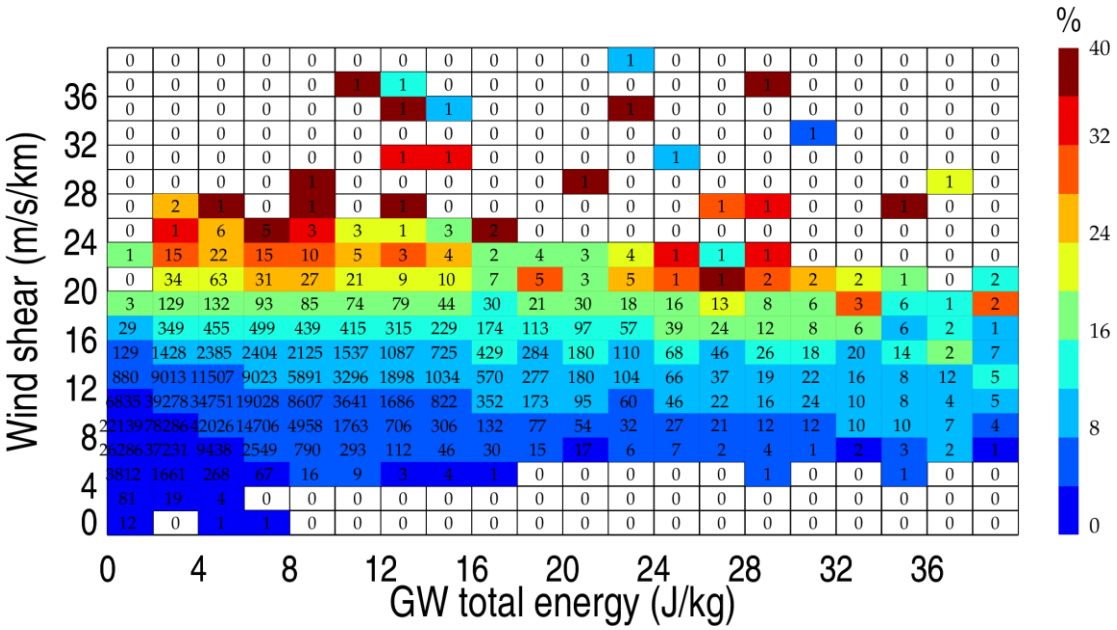

Figure S6. The joint distribution of *OF*(0<*Ri*<*Rit*) with GW energy and wind shear. The *OF*(0<*Ri*<*Rit*) and wind shear are derived from individual HVRRS profiles and vertically averaged over the tropospheric segment that is used for GW study. The numerical number indicates the matched profile number in each grid, using a bin size of 2 J/kg along the x axis and 2 m/s/km along the y axis.

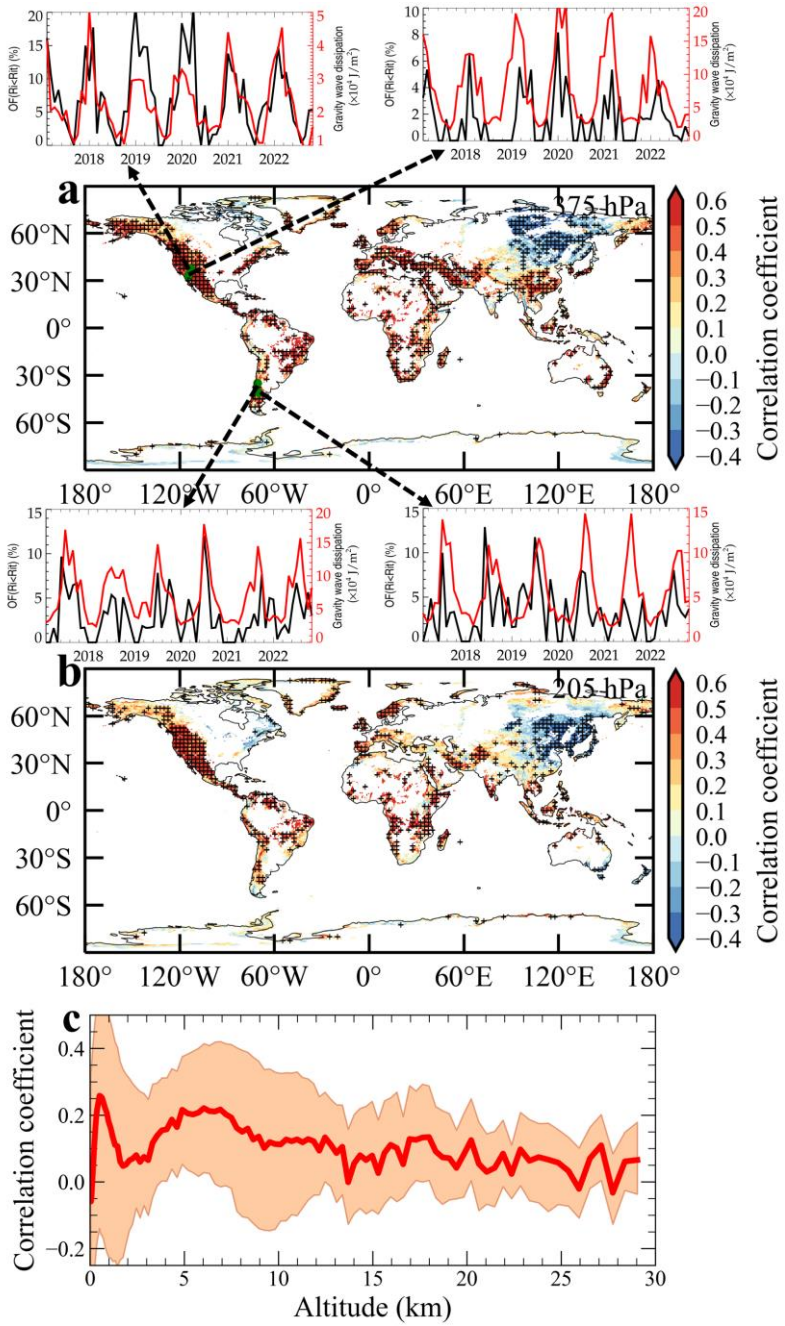

Figure S7. The correlation coefficient between monthly averaged ERA5-based orographic GW dissipation and monthly ERA5-based *OF*(*Ri*<*Rit*) at pressure levels of 375 hPa (a) and 205 hPa (b) during time period of January 2017 to October 2022. where plus signs indicate that the values are statistically significant (p<0.05). Four subplots around (a) display the monthly variation of orographic GW dissipation (red) and *OF*(*Ri*<*Rit*) (black) over two grids of the Rocky Mountain and two grids of the Andes Mountain. The coefficient at continuous heights from the ground up to 30 km is further displayed in (c), where the light red shadow denotes a significance of 95%.

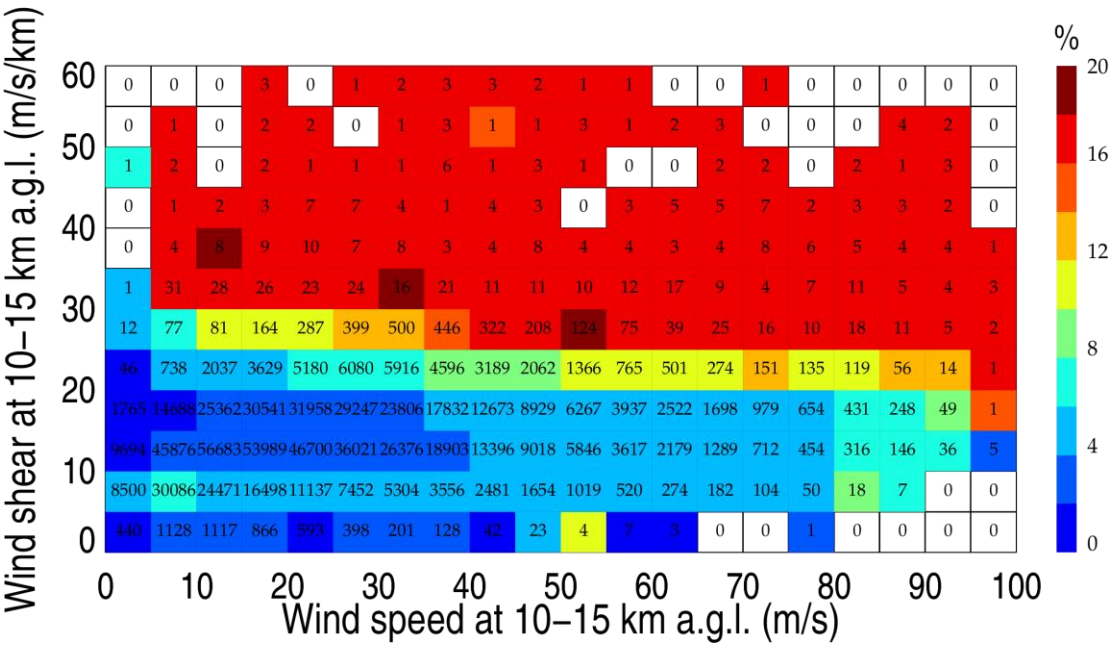

Figure S8. Joint distribution of HVRRS-derived wind speed, wind shear, and *OF*(0<*Ri*<*Rit*), with a bin size of 5 m/s along the x axis and 5 m/s/km along the y axis. Note that all the relationship is based on the mean result of individual profiles at heights of 10–15 km a.g.l.. The number indicates the matched profile number in each grid.

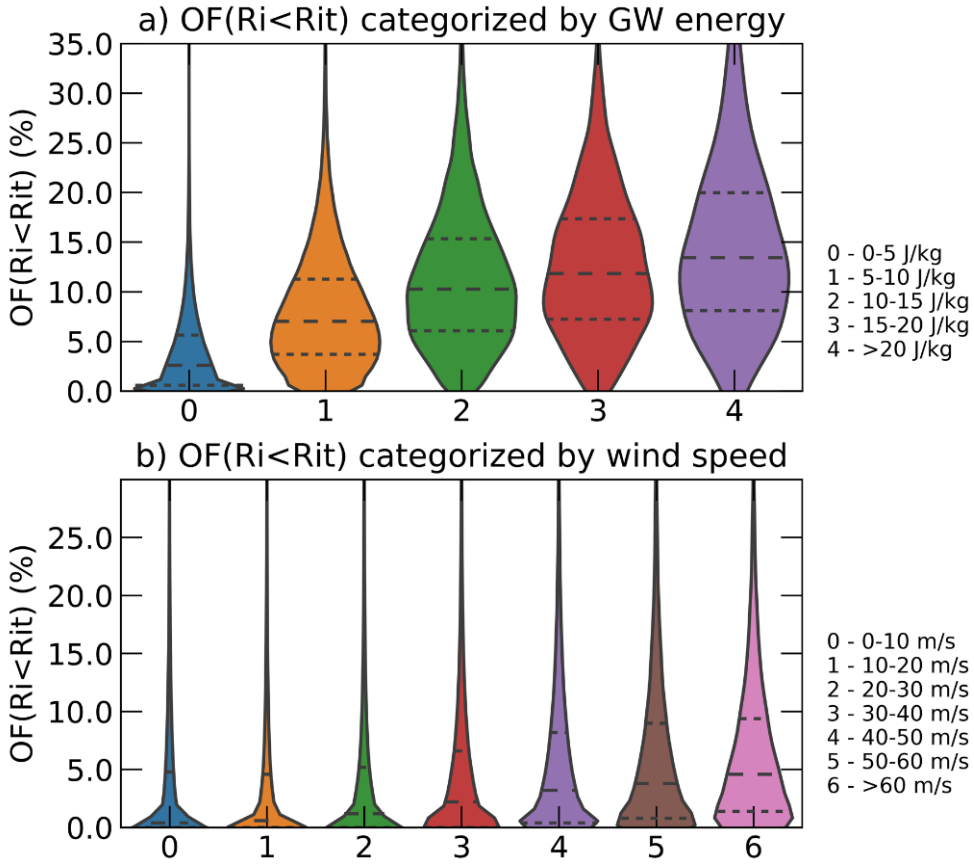

Figure S9. Violin plots of *OF*(*Ri*<*Rit*) categorized by GW total energy (a) and wind speed (b).